

Spatial distribution of electron-hole droplets in silicon

M. A. Tamor and J. P. Wolfe

Physics Department and Materials Research Laboratory, University of Illinois at Urbana-Champaign, Urbana, Illinois 61801

(Received 20 August 1979)

We report the first determination of the electron-hole liquid-distribution resulting from point laser excitation of Si. A cloud is observed with volume increasing nearly linearly with laser power, resulting in an almost constant average pair density. The cloud is slightly anisotropic in shape and is most dense at a point well within the crystal. The average pair density in the cloud is found to be 0.5% of the spectroscopically determined density of the liquid phase, $n_{eh} = 3.3 \times 10^{18} \text{ cm}^{-3}$. The low average density indicates that the luminescence distribution is due to a diffuse cloud of discrete droplets which occupy a small fraction of the total cloud volume. The size and density characteristics of the cloud are consistent with earlier phonon-wind models for Ge, which propose a nonequilibrium phonon flux as the dominant droplet-transport mechanism.

In pure Si or Ge at low temperatures, photoexcited carriers condense into an electron-hole liquid.¹ In Ge it has been shown that point-laser excitation, absorbed at the sample surface, produces a cloud of electron-hole droplets (EHD), each 1 to 10 μm in size and with carrier density $n_{eh} = 2.3 \times 10^{17} \text{ cm}^{-3}$. While the size of the cloud (up to ~ 4 mm) and droplet-filling factor ($\sim 1\%$) have been known for some time, only recently has the mechanism of droplet transport into the sample come into focus. Keldysh² proposed that a nonequilibrium flux of phonons—a “phonon wind”—could propel droplets macroscopic distances. This idea has been experimentally supported by Bagaev *et al.*³ and Hensel and Dynes,⁴ who observed the transport of drops away from a heat source and by Doehler, Mattos, and Worlock,^{5,6} who measured the velocity of droplets in the cloud. Greenstein and Wolfe⁷ made a direct connection between phonons and cloud formation by infrared imaging of droplet luminescence. They correlated cloud shape with anisotropies in both the phonon-flux and the absorption of phonons by drops. Both phonons from carrier thermalization in the excitation region (T phonons) and recombination-related R phonons may contribute to droplet transport.

In Ge, it has been observed by several methods that the average cloud density for point excitation is only weakly dependent on input power.⁸⁻¹⁰ This puzzling and unexpected feature can also be understood in terms of a phonon-wind mechanism. Bagaev *et al.*³ calculate the average pair density $n(r)$ in the cloud at a distance r from an isotropic source of phonons at the excitation point. They obtain $n(r) = n_0 \exp(-r/L_{eff})^3$, where L_{eff} is a characteristic distance dependent on the phonon source strength. The central density n_0 is independent of

power, and the cloud volume L_{eff}^3 expands linearly with phonon flux and therefore with excitation power. Markiewicz¹¹ recently included the effects of the recombination phonons to calculate the cloud size as a function of excitation power. He has found that the relative amounts of T and R phonons determine the absolute size of the cloud for a given power level and excitation spot size, but that above some threshold a linear dependence of cloud volume on power is still expected. Only for the case of no T phonons at all does the cloud fail to grow.

For several reasons there have been no spatial measurements of EHD in Si comparable to those done in Ge. Spectroscopic studies have well characterized the liquid parameters,^{12,1} and there is evidence for discrete drops,¹³ but spatial properties of the liquid distribution have not been reported. The experimental difficulty stems from the high density of e-h pairs within the Si EHD, $n_{eh} = 3.3 \times 10^{18} \text{ cm}^{-3}$. This causes the lifetime of EHD in Si to be very short (140 nsec versus 40 μsec in Ge), and the quantum efficiency for radiative recombination to be very low ($\sim 10^{-4}$) due to nonradiative processes. These factors predict a cloud in Si which is both smaller and less intense than that in Ge.

In this paper we describe experiments that characterize the liquid distribution in Si. We have determined the cloud size and shape and can estimate the average pair density and droplet velocities for the first time. Spectrally resolved images of the droplet cloud were obtained by combining photon-counting techniques with a computer-controlled scanning system, as diagrammed in Fig. 1. The high-purity Si sample ($N_A - N_D \leq 10^{12} \text{ cm}^{-3}$) with all (100) edges was immersed in a liquid-He bath at $T = 2 \text{ K}$. The sample was optically excited

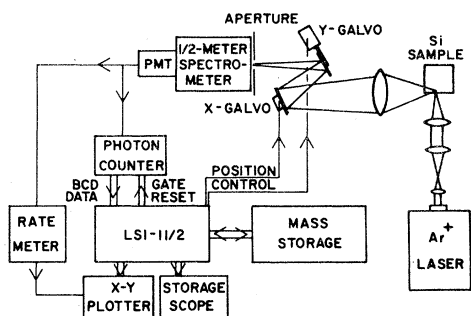


FIG. 1. Computer-controlled photon-counting imaging system with spectral resolution.

with a focused Ar^+ laser ($\lambda = 0.515 \mu\text{m}$) and the droplet luminescence at $\lambda = 1.15 \mu\text{m}$, selected by a $\frac{1}{2}$ spectrometer, was detected with an infrared sensitive photomultiplier tube.¹⁴ Spatial resolution was obtained by focusing a $5\times$ magnified crystal image onto a small aperture ($125\text{-}\mu\text{m}$ diam) at the entrance to the spectrometer. The image was translated by a pair of galvanometer-driven mirrors. The imaging process was controlled by a minicomputer which scanned the mirrors and recorded the luminescence intensity on a floppy-disk medium. An image consisted of a 256×256 array of integers, and typically took about 15 min to accumulate. The digitized image could be quickly replayed on a storage oscilloscope and photographed, as well as quantitatively analyzed as described below.

An analog representation of the image was obtained by plotting successive horizontal scans, shown in Fig. 2. This is a side view of the crystal as defined in the insert. For this absorbed laser power, $P_{\text{abs}} = 220 \text{ mW}$, the cloud extends into the crystal about 0.4 mm . The cloud shape is graphically displayed in Fig. 3(a) by contour mapping the luminescence intensity onto alternating light and dark bands, each border defining a line of constant intensity. This map shows two important features: (1) The maximum luminescence intensity and thus droplet density, occurs about $50 \mu\text{m}$ inside the sample, rather than at the surface, and (2) an anisotropy in the shape of the EHD cloud is visible, especially near the perimeter. Figure 3(b) is a contour map of a face view of the cloud, viewing into the laser beam which is completely absorbed by crystal. The cloud shows none of the anisotropies observed in Ge.⁷

For determining the gross characteristics of the cloud, the aperture was replaced with a vertical $50\text{-}\mu\text{m}$ slit and the total luminescence through this slit was recorded as the face-view image was translated horizontally. Typical scans are shown

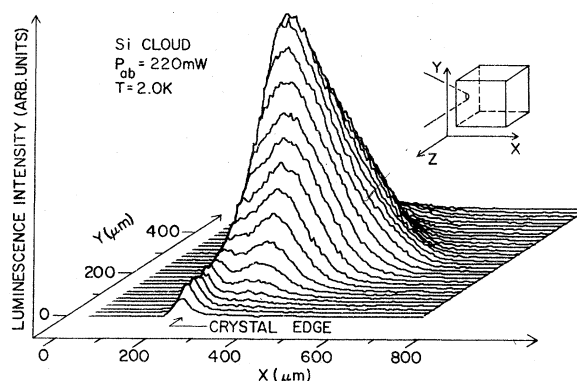


FIG. 2. Intensity plot of the EHD cloud luminescence at $\lambda = 1.15 \mu\text{m}$. The crystal edge is clearly visible in the foreground, and the intensity peak occurs about $50 \mu\text{m}$ inside. The peak intensity corresponds to 6×10^4 photon counts per second, or about 600 counts per image element. The excitation surface was etched, and the viewing surfaces polished.

in Fig. 4. From these slit scans the size and intensity of the EHD cloud was measured over $3\frac{1}{2}$ decades in laser power. Figure 5(a) displays the power dependence of the full width at half maximum, Δ , of the cloud. The product of full width and the peak intensity, $I_p \cdot \Delta$, is good measure of the total cloud intensity. This quantity, plotted in Fig. 5(b), varied nearly linearly with laser power, indicating that the droplet-production efficiency ϵ is quite independent of excitation level over this range. Below 1.0 mW , the cloud was the size of the laser spot, i.e., about $35 \mu\text{m}$ for a single laser line at $\lambda = 0.515 \mu\text{m}$. From 1 mW to the maximum power of 800 mW , the full width varied as $P_{\text{abs}}^{0.3}$. A discontinuity in the data occurred near $P_{\text{abs}} = 50 \text{ mW}$ with the onset of a He-gas bubble on the crystal surface. This local heating effect did not appear for the larger ($110\text{-}\mu\text{m}$) multiline laser spot, and the cloud expansion with power resumed along the same $P_{\text{abs}}^{0.3}$ curve.

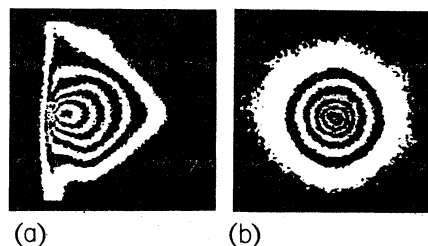


FIG. 3 (a). Contour map of the side view in Fig. 2. The apparent curvature of the crystal edge is due to the relative brightness of the cloud. (b) Face view of the cloud with $P_{\text{abs}} = 220 \text{ mW}$. This is the yz face in the insert of Fig. 2. Both photographs are $600 \mu\text{m}$ edge to edge.

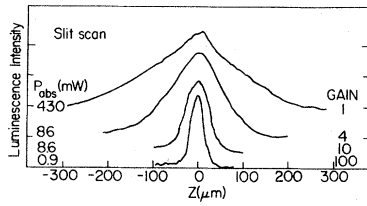


FIG. 4. Slit scans of the electron-hole liquid distribution at $\lambda=1.15 \mu\text{m}$ and $T=2 \text{ K}$. Total spatial resolution was about $20 \mu\text{m}$.

An estimate of the average e-h pair density can be obtained from these data, given droplet lifetime. We have measured a lifetime $\tau=140 \text{ nsec}$ for the droplet luminescence after the laser is switched off.¹⁵ The total number of pairs in droplets is given by $N=\epsilon P_{\text{abs}}\tau/h\nu$, where $h\nu$ is the photon energy. The average pair density in the cloud can be parametrized as $n_{\text{av}}\equiv N/\Delta^3$. A plot of n_{av}/ϵ

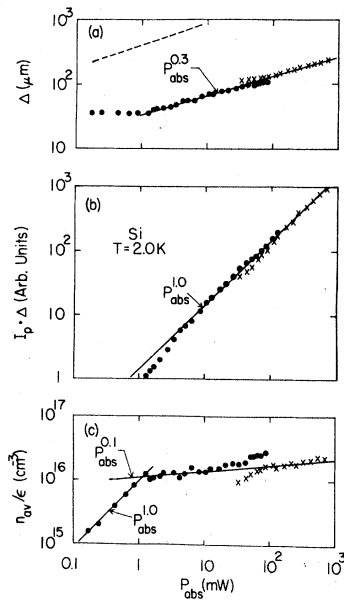


FIG. 5 (a). Cloud full width Δ as a function of absorbed laser power. The slope of 0.3 indicates that the cloud volume varies almost linearly with power. In all of these figures, solid circles indicate single laser line and the \times 's higher power, multiline excitation. (b) Power dependence of the total cloud intensity, with I_p the peak intensity of the cloud profile, as in Fig. 4. (c) Average pair density of the cloud as defined in the text. The abrupt change in slope at $P_{\text{abs}}=1.0 \text{ mW}$ indicates the power above which the laser spot size no longer limits the cloud size.

is given in Fig. 5(c). At low excitation levels, where the cloud size is determined by the laser spot size, the average pair density increases approximately linearly. At intermediate powers where the cloud is expanding, the density is relatively constant, varying by only a factor of 2 as the volume Δ^3 increases by a factor of 300. Variations in P_{abs}/Δ^3 near 50 mW correspond to a change in cloud shape due to either heating (single line) or increased spot size (multiline). Assuming a production efficiency $\epsilon=1$, the mean density $n_{\text{av}}=1.5 \times 10^{16} \text{ cm}^{-3}$ corresponds to a cloud filling factor of about 0.5%. This low average density clearly indicates that the cloud is a diffuse distribution of droplets which occupy only a small fraction of the total volume. For comparison with Ge, the dashed curve in Fig. 4(a) shows Δ from Ref. 16. For comparable power levels, the cloud size is an order of magnitude smaller in Si. By the same analysis as above, a filling factor of 1% is obtained for Ge.⁹

Under the assumption that a droplet created near the excitation region undergoes an exponential volume decay as it moves into the crystal, we can also estimate the average droplet velocity $v_{\text{av}}\equiv \frac{1}{2}\Delta/\tau$. For our measured range of Δ the average velocity varies between $1.2 \times 10^4 \text{ cm/sec}$ at low power and $7.5 \times 10^4 \text{ cm/sec}$ at high power, considerably larger than the $10^3\text{--}10^4 \text{ cm/sec}$ reported for Ge.^{5,6,7}

The slight anisotropy observed in the side-view image in Fig. 3(a) suggests the presence of phonon focusing, due to channeling of slow TA phonons along the $\langle 100 \rangle$ axis. However, the lack of anisotropy in the face view of Fig. 3(b) is in contrast to the large anisotropies observed for the cloud in Ge. This may be partly explained by the much smaller cloud size relative to the laser spot (up to $7\times$ compared to $40\times$ in Ge).⁷ In Ge the anisotropy has been attributed to T phonons localized near the excitation region. Other experiments⁶ and theories for Ge have supported the presence of R phonons which emanate from the droplets themselves. In silicon the R phonon contribution should be much greater than in Ge, since (a) Auger recombination is about $300\times$ faster, and (b) the average pair density of the cloud is nearly $50\times$ larger. Thus it seems likely that the dominance of R phonons, diffusely emitted from all droplets in the cloud, could explain the observed lack of anisotropy.

These experiments have characterized the EHL cloud in Si for the first time and indicate that the cloud is diffuse distribution of discrete droplets. The qualitative result that above a definite threshold power the cloud volume increases nearly linearly lends strong support to a phonon-wind model of droplet transport in Si.

We wish to thank E. E. Haller for supplying the Si crystal, M. W. Klein for the loan of his special photomultiplier tube, and M. Greenstein for his general help and suggestions. This project was

supported by the National Science Foundation under the MRL Grant No. DMR-77-23999. The computer system essential to these experiments was provided by NSF Grant No. DMR-77-11672.

-
- ¹See for example, the reviews by J. C. Hensel, G. A. Thomas, T. G. Phillips, and by T. M. Rice, in *Solid State Physics*, edited by H. Ehrenreich, F. Seitz, and D. Turnbull (Academic, New York, 1977), Vol. 32.
- ²L. V. Keldysh, *Pis'ma Zh. Eksp. Teor. Fiz.* **23**, 100 (1976) [*JETP Lett.* **23**, 86 (1976)].
- ³V. S. Bagaev, L. V. Keldysh, N. N. Sibel'din, and V. A. Tsvetkov, *Zh. Eksp. Teor. Fiz.* **70**, 702 (1976) [*Sov. Phys.—JETP* **43**, 363 (1976)].
- ⁴J. C. Hensel and R. C. Dynes, *Phys. Rev. Lett.* **39**, 969 (1977).
- ⁵J. Doehler, J. V. C. Mattos, and J. M. Worlock, *Phys. Rev. Lett.* **38**, 726 (1977).
- ⁶J. Doehler and J. M. Worlock, *Solid State Commun.* **27**, 229 (1978).
- ⁷M. Greenstein and J. P. Wolfe, *Phys. Rev. Lett.* **41**, 715 (1978).
- ⁸Ya. E. Pokrovskii and K. I. Svistunova, *Fiz. Tverd. Tela* **16**, 3399 (1974) [*Sov. Phys.—Solid State* **16**, 2202 (1975)].
- ⁹M. Voos, K. L. Shakley, and J. M. Worlock, *Phys. Rev. Lett.* **33**, 1161 (1974), also obtain $n_{av} \approx 10^{15} \text{ cm}^{-3}$ by a different method.
- ¹⁰B. J. Feldman, *Phys. Rev. Lett.* **33**, 359 (1974); G. W. Kamerman and B. J. Feldman, *Phys. Rev. B* **13**, 5615 (1976).
- ¹¹R. S. Markiewicz, unpublished.
- ¹²Ya. E. Pokrovskii and K. I. Svistunova, *JETP Lett.* **9**, 261 (1969). Ya. E. Pokrovskii, *Phys. Status Solidi A* **11**, 385 (1972).
- ¹³M. Capizzi, M. Voos, C. Benoit à la Guillaume, and J. C. McGroddy, *Solid State Commun.* **16**, 709 (1975).
- ¹⁴A Varian VPM-164 cooled to 190 K.
- ¹⁵This is close to other reported measurements, e.g., J. D. Cuthbert, *Phys. Rev. B* **4**, 1552 (1970). Our measured decay was somewhat nonexponential.
- ¹⁶J. P. Wolfe, R. S. Markiewicz, S. M. Kelso, J. E. Furneaux, and C. D. Jeffries, *Phys. Rev. B* **18**, 1479 (1978).

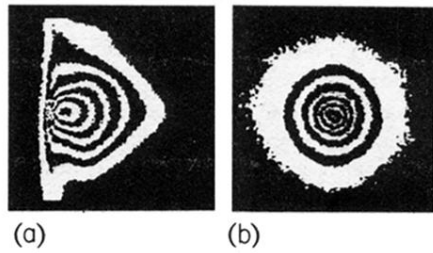


FIG. 3 (a). Contour map of the side view in Fig. 2. The apparent curvature of the crystal edge is due to the relative brightness of the cloud. (b) Face view of the cloud with $P_{\text{abs}} = 220$ mW. This is the yz face in the insert of Fig. 2. Both photographs are $600 \mu\text{m}$ edge to edge.